MNRAS **000**, 1–6 (2018) Preprint 1 April 2022 Compiled using MNRAS LATEX style file v3.0

The assembly of cosmic structure from baryons to black holes with joint gravitational-wave and X-ray observations

Sean McGee[1], Alberto Sesana[1,2], Alberto Vecchio[1,2]
[1]*School of Physics and Astronomy, University of Birmingham, Birmingham, B15 2TT, United Kingdom*
[2]*Institute for Gravitational Wave Astronomy, University of Birmingham, Birmingham, B15 2TT, United Kingdom*

Accepted . . . Received . . . ; in original form . . .

arXiv:1811.00050v1 [astro-ph.HE] 31 Oct 2018

ABSTRACT

The evolution of structure, how the first black holes form and grow and the environments and baryonic content in which they reside remain largely outstanding questions in astrophysics and fundamental physics. They will be the focus of major observational programmes in the coming decade(s), using different probes to reconstruct a full picture of the physical processes at work. In particular, the X-ray Athena mission and the gravitational-wave Laser Interferometer Space Antenna (LISA) offer two independent and complementary angles to tackle these problems. Here we explore some of the science opportunities that would open up if observatories with capabilities comparable to Athena and LISA were to operate simultaneously, and not in different epochs as currently planned. We show that at least a handful of systems containing a massive black hole in the mass range $\sim 10^5 - 10^8\,M_\odot$ discovered by LISA at redshift $\approx$ 1-to-5 could be monitored by Athena in an exposure time up to 1 Ms if prompt X-ray emission at the level of $\sim 0.1\% - 10\%$ of the Eddington luminosity is present. We also show that Athena can plausibly detect diffuse X-ray emission from the hot gas of the environment hosting a $\sim 10^8\,M_\odot$ massive black hole binary at $z \lesssim 1$. The large uncertainties reflect the poor theoretical understanding of these complex physical processes, which in turn emphasises the vast discovery space that these joint observations would access, and therefore the potential for significant discoveries and surprises.

Key words: gravitational waves – black hole physics – galaxies: formation and evolution

1 INTRODUCTION

The Laser Interferometer Space Antenna (LISA, Amaro-Seoane et al. 2017) is an ESA space-based gravitational-wave (GW) observatory that shall survey the gravitational-wave sky discovering black holes in the mass range from $\sim 10\,M_\odot$ to $\sim 10^7\,M_\odot$ up to redshifts ≈ 20 (Klein et al. 2016). LISA therefore provides a wealth of targets for exploring and characterising the environments in which black holes form, grow and merge, offering a so-far totally unexplored route to follow structure formation through cosmic time. LISA, however, will be totally blind to the properties of the environment in which black holes reside, and the associated properties of baryons and gas. To study them an X-ray telescope capable of deep wide-field imaging and spatially-resolved spectroscopy, which are features of the next generation X-ray telescopes, such as ESA's Athena mission (Nandra et al. 2013), are needed. Combined with optical and radio observations, through e.g. the Large Synoptic Sky Survey (LSST; LSST Science Collaboration et al. 2009) and the Square-Kilometre-Array (SKA; Dewdney et al. 2009), the next decades are well set to provide major advances, and likely big surprises, in the study of these phenomena.

Athena and LISA are currently scheduled to operate sequentially, therefore preventing simultaneous observations of the same systems in these two radically different observational bands. Progress will therefore rely on understanding these objects and environments independently, and on characterising their properties through statistical studies of the catalogues of the two missions. An interesting question to consider, which is at the centre of this paper, is: If observatories with capabilities comparable to LISA and Athena were to operate simultaneously, what is the potential of observing the same systems, and the associated phenomena in these two bands?

There are three obvious science targets that could provide unprecedented information about major open questions in astrophysics and cosmology: (i) the assembly history of structures throughout cosmic time as tracked by (super-)massive binary black hole binary (MBHB) mergers (Volonteri et al. 2003; Sesana et al. 2004); (ii) the massive black holes and their environment in the low-redshift universe, revealed by LISA surveys of extreme-mass-ratio inspirals (EMRIs, Barack & Cutler 2004; Amaro-Seoane et al. 2007); and (iii) the environment and possible high-energy phenomena associated with (heavy) stellar-mass binary black holes (BBHs) in the local universe (Sesana 2016). We will explore them in turn in the next section.

Investigating whether it is possible to make joint GW-X ray observations of the same environment boils down to answering the

© 2018 The Authors

following questions: if a BH is detected by LISA, is it feasible to carry out a targeted follow-up X-ray observational campaign covering the whole GW position error-box on the sky? And in turn how deep can the X-ray observations go (and therefore what fraction of GW-detected events could they reach) either to detect prompt X-ray emission following the merger, or diffuse X-ray emission from the surrounding environment? The answer to these questions depends on the performances of the instruments at one's disposal and, possibly more significantly, on the actual details of physical processes at work, which currently are largely uncertain (see, e.g., Armitage & Natarajan 2002; Milosavljević & Phinney 2005; Chang et al. 2010; Palenzuela et al. 2010; Bode et al. 2010; Gold et al. 2014; Cerioli et al. 2016; Tang et al. 2018; d'Ascoli et al. 2018). These uncertainties in turn reflect the substantial discovery space that these observations will access.

As reference performance of a GW instrument we consider the current design of the LISA mission. A 2.5 million-km arm interferometer in heliocentric orbit with operational requirements as described in Amaro-Seoane et al. (2017) (corresponding to the noise spectral density of their Fig. 2). For the X-ray observatory we use the design specifications of the Athena WFI detector (Rau et al. 2013). We assume a field of view of 0.4 deg^2 and a flux sensitivity for a 5σ detection in an integration time T of

$$F_X = 3\times10^{-17}\left(\frac{10^6\,\mathrm{sec}}{T}\right)^{1/2}\mathrm{erg\,cm^{-2}\,s^{-1}}. \quad (1)$$

In absence of solid predictions, in this feasibility study we use Eddington luminosity, $L_{\rm Edd} = 1.26\times10^{38}\,(M/M_\odot)\,\mathrm{erg\,s^{-1}}$ as a proxy for the possible prompt X-ray emission associated to a merger of a binary black hole. We assume that 10% goes into X-ray (e.g. Lusso et al. 2010) and that the typical X-ray spectrum is a power law with spectral index of 0.7, consistent with the power-law found for quasars (Reeves & Turner 2000). The luminosity is integrated in the hard-X band so that the results shown are independent on obscuration due to photoelectric absorption up to a column density $10^{23}\,\mathrm{cm^{-2}}$. For the diffuse X-ray emission from the hot gas in the environment we will discuss our assumptions in the next section.

2 THE ASSEMBLY OF MASSIVE BLACK HOLE BINARIES AND THEIR HOSTS

LISA will track the assembly history of SMBHs throughout cosmic time by detecting binary mergers of systems in the (rest-frame) mass range $\sim 10^3 - 10^7\,M_\odot$ anywhere in the Universe, reaching redshift $z\approx20$ and beyond, if such systems are present (Amaro-Seoane et al. 2017). The detection rate is uncertain, in the range $\sim 10-1000$ for a planned 4 year mission duration (Klein et al. 2016). The mass-redshift distribution of the observed systems is subject to large uncertainties, and based on modelling, the majority of the detections will be of systems with masses $\lesssim 10^5 M_\odot$ at redshift $z\gtrsim5$, although a few detections of black holes with masses $\gtrsim 10^6 M_\odot$ at $z\lesssim2$ are expected. This is a quite extraordinary sample of objects, selected in a radically different way from AGN and/or time-domain surveys.

The first step is to identify the performance of LISA in observing MBHBs. For the problem at hand there are two quantitative indicators of the performance: the signal-to-noise ratio (S/N) at which a binary of a given mass and redshift can be observed and the error-box in the sky associated with the detection. The specific numbers for a given system depend on a large number of factors that introduce many complications that prevent us from giving a clear-cut picture of the science potential of these observations and go beyond the scope of this work in which we look at broad order of magnitude results. In this spirit, to derive an empirical relation between the total mass of the MBHB M and the S/N, ρ, at which it is observed, we consider the set of simulations performed by Klein et al. (2016). They are based on population models from Barausse (2012), which feature different seed BH formation and subsequent accretion histories, also resulting in a wide range of spin and mass ratio distributions. We include all the observed systems in all models and we find the median angular resolution $\Delta\Omega$ is related to the median S/N, ρ, at which a system is observed by

$$\Delta\Omega \approx 0.5\left(\frac{\rho}{10^3}\right)^{-7/4}\mathrm{deg}^2. \quad (2)$$

Note that the relation is slightly flatter than the standard $\Delta\Omega\propto\rho^{-2}$ dependency. This is due to the fact that larger ρ are generally obtained for more massive binaries, which tend to stay in band for a shorter time. The scatter around the median is large, 0.7dex, and is found to be dominated by the range of source sky location, inclination and polarization angles, rather than the individual mass, mass ratios and spin values of the systems.

With a scaling in hand, we compute the sky-inclination-polarization averaged S/N for an equal-mass MBHB as a function of M and z, using the latest LISA sensitivity curve (Amaro-Seoane et al. 2017) and PhenomC waveforms for non-spinning, circular binaries (Santamaría et al. 2010). To each (M,z) pair we can then associate a median sky localization through Eq. (2). Although the scaling was obtained from a binary population featuring more complex properties than the systems used to compute S/N's on the mass–redshift grid, we note that the distribution of MBHB mass ratios in Klein et al. (2016) peaks at unity; moreover the exact spin value does not have a major impact on the S/N calculation which makes the use of non spinning waveforms acceptable. Contour plots of median $\Delta\Omega$ in the (M,z) plane are shown in green scale in Fig. 1.

We can now turn to the question of whether any X-ray radiation could be observed, and we consider two scenarios: i) a prompt emission triggered at the merger, and ii) diffuse X-ray emission

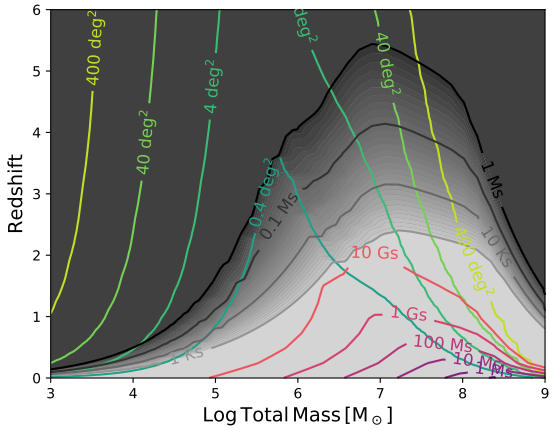


Figure 1. Feasibility of joint GW/X-ray observations of MBHB mergers in the mass-redshift plane. Green-yellow contours mark the median sky location accuracy (in deg^2) of mergers achievable by LISA observations. Grey shaded contours represent the total exposure time needed by Athena to cover the corresponding LISA error-box, assuming 10% Eddington-limited accreting MBH. Red-purple lines denote the exposure needed to detect diffuse X-ray emission from the merger host (see main text for details).

from the hot gas surrounding the dense environment in which the binary resides.

We start by considering point-like emission resulting from the merger. With the assumptions made in the previous section, the emission is in the X-ray band is $L_X \approx 1\times10^{43}\,(M/10^6\,M_\odot)$erg s^{-1}. For any LISA source mass and redshift, we can then compute the X-ray flux and, via Eq (1), the integration time required to achieve a 5σ detection in a single pointing. Finally we obtain the required total observations time by combining the number of pointing needed to cover the GW error box, i.e. we multiply by $\Delta\Omega/0.4\,\mathrm{deg}^2$. In our analysis we therefore implicitly assume that the emission is persistent at a roughly constant level over the Athena's observation time, which might be the case if there is enough gas in the vicinity of the binary to light a quasar following its final coalescence (as found in some recent simulations, e.g., Tang et al. 2018). The integration time is shown in the (M,z) plane by the grey-colour map in Fig. 1.

It is interesting to note that Athena has the potential to detect a counterpart of a $\sim 10^6-10^7 M_\odot$ merging binary radiating at 10% Eddington out to $z\approx2$ in less than 10 pointings for a total integration time of less than 1ks. Note that for such masses, the dynamical timescale at merger is of the order of 1ks as well, implying that a bright X-ray transient of similar duration might be plausible. Such transient would be prompted by "gas squeezing" and might be highly super-Eddington (Armitage & Natarajan 2002; Cerioli et al. 2016), facilitating detection by Athena at even larger z. Reaching out to $z=4(5)$ would generally require several pointings for a total time of 100ks(1Ms). We note however that these results assume the 'median value of sky localization'. Because of the large scatter in Eq. (2), for example, the 10% best localized LISA sources can be followed-up by Athena up to twice the redshift shown in Fig. 1 (see Sec. 5).

We turn now to the question of whether diffused X-ray emission from the gas contained in the structure which harbours the MBHB could be observed by Athena. In order to do this, we need to estimate, as a function of MBH's mass and redshift, the typical dark matter halo (DM) mass that hosts the MBHB identified through GWs. We use the semi-analytic model of Barausse (2012) that provides, for each merger, the mass of the DM halo of the largest structure in which it occurs. We group MBHBs in a mass-redshift grid and compute, at each grid point, the median of the largest DM halo associated with the merger. We fit the result with the relation

$$\log M_{\rm DM} = 11 + 0.15\,(\log M_{\rm BHB} - 3)^{1.7} - \log(1+z)^{1.2}\,. \qquad (3)$$

Note the non linear log-log relation between the halo and MBHB mass. As expected, host halos get larger at higher masses and lower redshifts. However, even for $10^7-10^8 M_\odot$ systems, typical halo masses are $\approx 10^{11}-10^{12} M_\odot$, consistent with mergers being hosted in small groups. In general, the presence of a large cluster in coincidence with a MBHB merger is rare, due to the exponential cutoff of the DM halo mass function at $M > 10^{14} M_\odot$. Also in this case, there is a significant scatter in the relation, and few mergers might occur in structures as massive as $\approx 10^{13} M_\odot$ (see supplementary material).

We can now relate the halo mass to the X-ray luminosity of the hot intra-cluster gas with (Anderson et al. 2015)

$$L_{X,\rm bol} = E(z)^{7/3} L_0 \left(\frac{M_{500}}{M_0}\right)^{\alpha} \qquad (4)$$

where $M_0 = 4\times10^{14} M_\odot$, $L_0 = 1.4\times10^{44}$erg/s, $\alpha = 1.85$, $E(z) = [(1+z)^3\Omega_M + \Omega_\Lambda]^{1/2}$ and M_{500} is the total mass enclosed in r_{500} (the radius within the average density of the halo is 500 times the average background density). M_{500} and r_{500} can be computed given $M_{\rm DM}$ and z, the luminosity can then be converted in surface brightness which can be compared to the WFI detection limit (surface brightness of 5×10^{-16} erg cm^{-2} s^{-1} arcmin^{-2} in 100ks, see Eq. (1)). The orange-red contours in Fig. 1 show integration times needed to detect diffuse emission from the halo hosting the merging binary. The figure highlights that although a detection is unfeasible for typical events, some low redshift ($z \lesssim 1$) and high mass systems ($M \sim 10^8 M_\odot$) may be observable, see also Sec. 5.

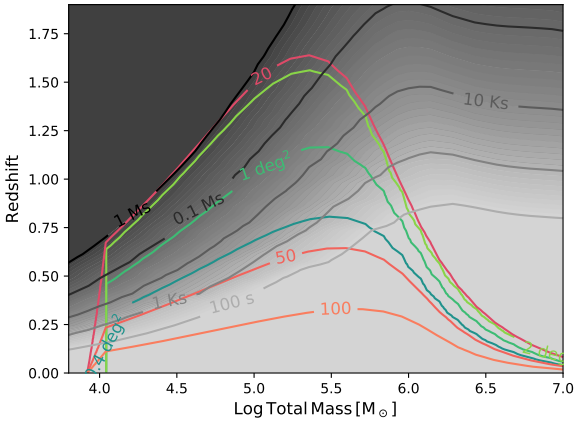


Figure 2. Feasibility of joint GW/X-ray observations of a massive black hole identified through GW observations of a stellar compact object (here assumed to be a $10\,M_\odot$ BH) spiralling into a massive companion (EMRI) in the MBH mass-redshift plane. Red contours indicate the signal-to-noise ratio of LISA detections. Green-yellow contours mark the associated size of the median error box in the sky containing the GW source. Grey shaded regions are the exposure time for Athena observations to detect a 10 % Eddington accreting source.

3 THE LOW-MASS END OF THE MASSIVE BLACK HOLE MASS FUNCTION

LISA will also map populations of MBHs at low redshift (up to $z\approx2$) through the detection of low-mass compact objects (neutron stars and stellar-mass BHs) spiralling into them; the so-called extreme mass ratio inspirals (EMRIs Amaro-Seoane et al. 2007). Also in this case, the event rate is highly uncertain, ranging from just a handful to possibly thousands during the mission lifetime (Babak et al. 2017). Most of of these systems will be characterised by MBH masses of $\lesssim 10^6 M_\odot$, therefore probing a region of the MBH parameter space very poorly known (Gair et al. 2010). Note that standard EMRI formation channels are not related to MBH accretion (see Amaro-Seoane et al. 2007, for a review), which will allow us to access a sizable sample of the completely unexplored low mass quiescent MBH population, inaccessible, by definition, to electromagnetic observations.

Similarly to the MBHB case, we consider the depth of a GW observation as a function of the MBH mass, M (which is essentially the total mass of the system given the extreme mass ratio), in the (M,z) plane. We set the compact object companion to have a mass of $10M_\odot$. We then relate the typical GW sky error box to the detection S/N by considering the extensive set of simulations reported in Babak et al. (2017), for which we obtain the empirical fit:

$$\Delta\Omega \approx 0.05\,\mathrm{deg}^2\,\rho^{-5/2}, \qquad (5)$$

which relates the median sky resolution $\Delta\Omega$ to the median S/N ρ. Here the slope is steeper than ρ^{-2} (although the scatter, 0.4dex, is

still large). As for the MBHB case, we take a grid of points in (M,z), compute sky- and inclination-averaged ρ using AK waveforms assumiing a plunge eccentricity of $e_p = 0.2$ (consistent with Babak et al. 2017) and assign a median $\Delta\Omega$ based on Eq. (5). The results of this procedure are shown in Fig. 2 by the colour contours. There are two obvious differences with respect to the MBHBs case: events are observed only up to moderate redshifts $z \lesssim 2$, and the associated $\Delta\Omega$ is much smaller, of the order of 1 deg^2 or smaller. The largest uncertainty region shown corresponds to $\Delta\Omega = 2$ deg^2 which is the typical sky localization accuracy of a LISA threshold detection (assumed at $\rho = 20$).

Although EMRI formation is generally not associated with AGN activity (but see Levin 2007, for an alternative scenario), a fraction of EMRIs will nonetheless occur in AGNs. This is particularly interesting since the drag from the accretion disk might imprint an observable signature in the EMRI dynamics, thus informing us that the inspiral is occurring around an accreting MBH (Yunes et al. 2011; Barausse et al. 2014). We then evaluate what Athena may be able to reveal by assuming, as for the MBHB case, a bright source shining at 10% of its Eddington luminosity in the 0.5-10 keV band.

The total exposure needed to cover the LISA error-box is shown by the grey colour scale in Fig. 2. Note that most of the sources (if X-ray emission is present at this level) would be detected at the inexpensive cost of ≈ 1 ks of observing time. Exposures extending to ~ 1 Ms would therefore allow us to reach a sensitivity below 1% Eddington. Moreover, for a few percent of the detected EMRIs, the 3-dimensional error box from GW observations will be sufficiently small to contain just one Milky Way-like galaxy, allowing a much more systematic observational campaign with other facilities. On the other hand, diffuse X-ray emission from the galaxies hosting this class of GW sources is likely way beyond the reach of an Athena-class instrument. By applying the MBH-halo relation that we have presented in Section 2, Eq. (3) and Fig. 1, we find that the emission from the host would require, at best, several years of exposure time to be detected.

4 STELLAR MASS BINARY BLACK HOLES

LISA will be able to observe stellar-mass binary black holes (BBHs) many years before they coalesce (Sesana 2016), an event that will be observed by ground-based GW observatories. The time of the merger will be known in advance, with a statistical uncertainty of ≈ 1 sec and the sky location will be smaller than Athena field of view. In fact, taking the results of Del Pozzo et al. (2018), and considering only the BBHs observable by both LISA and ground-based GW instruments, we find that the median sky-localisation is

$$\Delta\Omega \approx 0.2\,\mathrm{deg}^2\,\rho^{-2}. \quad (6)$$

This will allow us to point in advance and stare at the site of a collision of BBHs when this catastrophic event takes place. Although progress is continuously being made for ground-based technology, and third-generation GW ground-based observatories (e.g. Punturo et al. 2010; Abbott et al. 2017) are expected to be in operation together with a space-based mission, it is unlikely that they will able to provide the necessary advanced warning to trigger X-ray observations, simply due to the short time these events are in band, $\approx 15.5\eta\,(f_{\rm low}/3\,{\rm Hz})^{-8/3}\,(M/20M_\odot)^{-5/3}$ min, where η is the symmetric mass ratio and $f_{\rm low}$ the low-frequency cut-off of the instrument's sensitivity window.

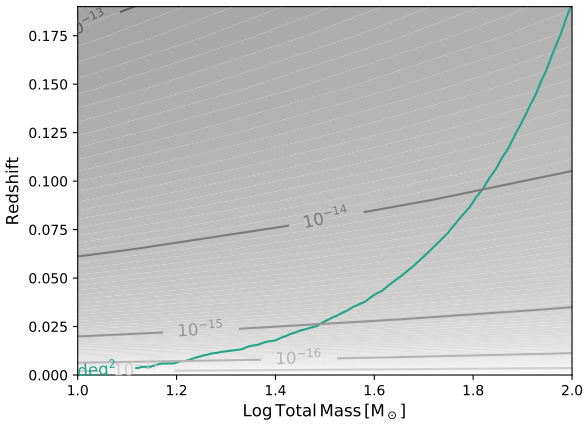


Figure 3. The discovery space in the total mass-redshift plane of joint GW/X-ray observations of stellar mass binary black holes. The green line marks the median LISA sky localisation accuracy corresponding to 0.4 deg^2, which corresponds to the Athena field of view, so that systems below this line can be followed-up in X-ray with a single pointing. Grey shaded contours represent the 5σ limit that an Athena non-detection will impose on the mass-energy conversion efficiency into X-ray ε (see text for details).

In general, BBHs are not expected to produce an electromagnetic signal. If the source was accreting at the Eddington limit, it would still produce a flux $\approx 10^{-17}(M/10M_\odot)\,(D_L/1\,{\rm Gpc})^{-2}$ erg s^{-1} cm^{-2}. Limits for e.g. GW150914 ($D_L \approx 400$ Mpc) have been set to an X-ray flux of $\approx 1 - 0.1 \times 10^{-9}$ in the 2-20 keV band (Kawai et al. 2017). A number of hypothetical scenarios have been put forward to produce bright supernovae precursors (Michaely & Perets 2018), prompt GRB emission (Perna et al. 2016) and luminous afterglows (de Mink & King 2017) of BBH mergers. In all cases, the emission would be strong enough that would be easily observable by Athena. Detection of bright emission from these objects will revolutionize our understanding of their formation, dynamics and environment.

Here, we take the standard assumption that the merger occurs approximately in vacuum. Even in this case, an X-ray telescope could still characterise this region well in advance of the merger, and therefore provide the deepest limit (or an actual detection) of radiation produced at the time of the merger.

A possible way of quantifying the sensitivity of an X-ray observation of these systems is to compute the limit on the conversion efficiency ε of the rest-mass of the system into electro-magnetic radiation. We assume, for simplicity, that all the electro-magnetic energy is released in X-rays, and that photons are emitted with energy E_γ uniformly distributed in the energy range $\Delta E_\gamma \sim E_\gamma$. The number of photons corresponding to an energy of Mc^2 is thus

$$N_\gamma \approx 10^{63}\left(\frac{M}{M_\odot}\right)\left(\frac{E_\gamma}{1\,{\rm keV}}\right)^{-1}. \quad (7)$$

Assuming isotropic emission, a source at a luminosity distance D_L and a collecting area of a wide field instrument $A_{\rm WFI}$, the number of photons impinging the X-ray detector is

$$N_{\rm WFI} = 10^{14}\left(\frac{M}{M_\odot}\right)\left(\frac{A_{\rm WFI}}{1\,{\rm m}^2}\right)\left(\frac{D_L}{300{\rm Mpc}}\right)^{-2}\ {\rm cts}. \quad (8)$$

If the burst is produced by some exotic mechanism associated to the formation of the remnant black hole, it will occur on the merger timescale, $\tau \sim 10^{-4}(M/M_\odot)$ s. The number of photons collected

during the burst has to be compared to the background level of the instrument integrated over the time τ. The irreducible background limit of Athena is expected to be at the level of

$$F_{\rm bkg} \approx 5 \times 10^{-3} {\rm cts\,cm^{-2} s^{-1} keV^{-1}}. \quad (9)$$

Using our simplifying assumption that photons are received in an energy interval ΔE_γ over the timescale τ, from Eq. (9) we obtain an average background count of

$$\bar{N}_{\rm bkg} \approx 0.5 \frac{M}{M_\odot} \left(\frac{\Delta E_\gamma}{1\,{\rm keV}}\right) \left(\frac{A_{\rm WFI}}{1\,{\rm m^2}}\right) {\rm cts}. \quad (10)$$

From BBHs with $M \gtrsim 10 M_\odot$, $\bar{N}_{\rm bkg} \gg 1$ and therefore we approximate the distribution as a Gaussian with variance $\bar{N}_{\rm bkg}$. We can achieve a 5σ detection for conversion efficiency as low as

$$\varepsilon_{\rm th} = \frac{N_{\rm min}}{N_{\rm WFI}} = 5 \times 10^{-14} \left(\frac{M}{M_\odot}\right)^{-1/2} \left(\frac{D_L}{300{\rm Mpc}}\right)^{-2}, \quad (11)$$

which is shown by the shaded grey scale in Fig. 3. Note that, since the number of emitted photons is $\propto M$ but the background contamination scales with $M^{-1/2}$, we get $\varepsilon_{\rm th} \propto M^{-1/2}$. This mean that, in principle, MBHB would be best suited to this test, compared to BBHs. Note, however the D_L^{-2} dependence, which makes BBHs much better candidates for this type of test. MBHBs are in fact mostly expected at luminosity distances of several Gpc, whereas BBHs observed by LISA (and then with ground-based observatories) may be as close as $D_L < 100$ Mpc. Therefore, the 2-3 orders of magnitude gained by MBHBs via the $M^{-1/2}$ scaling are likely to be overcame by the several (eight, for a source at $z = 2$) orders of magnitude loss due to the D_L^{-2} scaling.

5 SUMMARY

We have shown that an X-ray telescope of the Athena class has the potential of discovering X-ray emission from high-energy phenomena connected to black holes discovered by LISA through GW observations, ranging from stellar mass black holes in the local universe to massive black hole binary systems at redshift ≈ 5 and possibly beyond. Diffuse X-ray emission from the host galaxy/cluster will be much more difficult to detect, and is likely to be confined to systems at $z \lesssim 1$ that harbour MBHBs of mass $\sim 10^8 M_\odot$. As most of the binary systems detected by LISA are long-lived GW sources (where the radiation is first detected months-to-years in advance of the binary merger) an Athena class X-ray instrument will also have the opportunity of long "stares" at the relevant patch of the sky to characterise the environment in which these targets reside and monitor emerging transient X-ray radiation in real time if it is released by physical process associated to black hole binary mergers. The results presented here are affected by very considerable (by orders of magnitude) uncertainties in the underlying physical processes. If on the one hand the possibility of joint GW-X-ray observations should be approached with considerable cautiousness, on the other hand this highlights the tremendous opportunity of (possible multiple) discoveries and transformational observations.

ACKNOWLEDGEMENTS

SMG and AV acknowledge the support by UK's Science and Technology Facilities Council (STFC); AS is supported by a University Research Fellowship of the Royal Society. We thank E. Barausse for providing the MBHB population models discussed in the Appendix.

REFERENCES

Abbott B. P., et al., 2017, Classical and Quantum Gravity, 34, 044001
Amaro-Seoane P., Gair J. R., Freitag M., Miller M. C., Mandel I., Cutler C. J., Babak S., 2007, Classical and Quantum Gravity, 24, R113
Amaro-Seoane P., et al., 2017, preprint, (arXiv:1702.00786)
Anderson M. E., Gaspari M., White S. D. M., Wang W., Dai X., 2015, MNRAS, 449, 3806
Armitage P. J., Natarajan P., 2002, Astrophysical Journal, 567, L9
Babak S., et al., 2017, Phys. Rev. D, 95, 103012
Barack L., Cutler C., 2004, Phys. Rev. D, 69, 082005
Barausse E., 2012, MNRAS, 423, 2533
Barausse E., Cardoso V., Pani P., 2014, Phys. Rev. D, 89, 104059
Bode T., Haas R., Bogdanović T., Laguna P., Shoemaker D., 2010, Astrophysical Journal, 715, 1117
Cerioli A., Lodato G., Price D. J., 2016, MNRAS, 457, 939
Chang P., Strubbe L. E., Menou K., Quataert E., 2010, MNRAS, 407, 2007
Del Pozzo W., Sesana A., Klein A., 2018, MNRAS, 475, 3485
Dewdney P. E., Hall P. J., Schilizzi R. T., Lazio T. J. L. W., 2009, IEEE Proceedings, 97, 1482
Gair J. R., Tang C., Volonteri M., 2010, Phys. Rev. D, 81, 104014
Gold R., Paschalidis V., Ruiz M., Shapiro S. L., Etienne Z. B., Pfeiffer H. P., 2014, Phys. Rev. D, 90, 104030
Kawai N., Negoro H., Serino M., Mihara T., Tanaka K., Masumitsu T., Nakahira S., 2017, PASJ, 69, 84
Klein A., et al., 2016, Phys. Rev. D, 93, 024003
LSST Science Collaboration et al., 2009, preprint, (arXiv:0912.0201)
Levin Y., 2007, MNRAS, 374, 515
Lusso E., et al., 2010, A&A, 512, A34
Michaely E., Perets H. B., 2018, Astrophysical Journal, 855, L12
Milosavljević M., Phinney E. S., 2005, Astrophysical Journal, 622, L93
Nandra K., et al., 2013, preprint, (arXiv:1306.2307)
Palenzuela C., Lehner L., Liebling S. L., 2010, Science, 329, 927
Perna R., Lazzati D., Giacomazzo B., 2016, Astrophysical Journal, 821, L18
Punturo M., et al., 2010, Classical and Quantum Gravity, 27, 194002
Rau A., et al., 2013, preprint, (arXiv:1308.6785)
Reeves J. N., Turner M. J. L., 2000, MNRAS, 316, 234
Santamaría L., et al., 2010, Phys. Rev. D, 82, 064016
Sesana A., 2016, Physical Review Letters, 116, 231102
Sesana A., Haardt F., Madau P., Volonteri M., 2004, Astrophysical Journal, 611, 623
Tang Y., Haiman Z., MacFadyen A., 2018, MNRAS, 476, 2249
Volonteri M., Haardt F., Madau P., 2003, Astrophysical Journal, 582, 559
Yunes N., Kocsis B., Loeb A., Haiman Z., 2011, Physical Review Letters, 107, 171103
d'Ascoli S., Noble S. C., Bowen D. B., Campanelli M., Krolik J. H., Mewes V., 2018, Astrophysical Journal, 865, 140
de Mink S. E., King A., 2017, Astrophysical Journal, 839, L7

APPENDIX A

In Sec. 2 we presented results based on median properties of the GW-detected MBHBs. Here we provide some insight in what might be achieved by considering particularly favourable sources. Figure 4 is the same as Figure 1 but considering the best localised LISA sources, defined as the sources belonging to the tenth percentile of sky location distribution at each mass-redshift point. We see that now Athena could reach the merger remnant of a MBHB of $\sim 10^7 M_\odot$ – emitting 10% of its Eddington luminosity in the X-ray band – up to $z \approx 8$, and a significant portion of the $10^6 - 10^8 M_\odot$ and $z \approx 5-8$ region is accessible with ~ 1 Ms exposure time. For sources at redshift $z \approx 1-2$, with the same observing time one could probe X-ray emission down to $\sim 0.1\%$ of the Eddington limit, enabling the discovery and characterization of faint counterparts.

Detection of diffuse X-rays from the environment is still very unlikely. We note however that this conclusion is based on considering the median halo mass for a given mass-redshift point. Figure 5 shows the median, tenth and ninetieth percentiles of the host DM halo distribution for all mergers at $z < 1$ (black) and $2 < z < 3$ (red). It can be seen that about 10% of MBHBs with total mass $M \approx 10^7 M_\odot$ resides in halos that are a factor of ≈ 5 heavier then the mean. According to Eq. (3), this implies an increased X ray luminosity by a factor $\approx 10-20$. In turn, this implies that, for a given exposure, detection can be achieved for sources at 3-4 times larger distances than those shown in Figure 4. Diffuse X-ray emission from the hosts of merging systems with $M \approx 10^8 M_\odot$ at $z < 1$ might therefore be possibly detected by Athena in less than 1Ms, if they reside in favorably massive halos.

Finally, it is also interesting to compare the portion of the (M, z) parameter space covered by both LISA and Athena with some representative MBHB population models. This is shown in Figures 6 and 7 for two selected MBHB populations extracted from the semi-analytic model of Barausse (2012): these are the Q3 models used in Klein et al. (2016) featuring heavy seeds without (left) or with (right) MBHB merger delays due to the hardening phase. The yellow-red contours are $d^2N/(d\log M dz)$, the number of sources per unit (log) mass and redshift, for a 4-year LISA mission duration. Considering a maximum total exposure limit of 1Ms for Athena's observations, joint detections are potentially possible for several systems in both cases. These also include a few systems at $z < 2$, for which Athena will be sensitive to very sub-Eddington luminosities, as already discussed in the main text. Note that by considering the best 10% localized sources, the number of promising targets is only moderately extended to $z \approx 6$. This is because the best combination of LISA sky localization and Athena performance is achieved for $M \approx 10^7 M_\odot$, and such systems are relatively rare at these high redshifts.

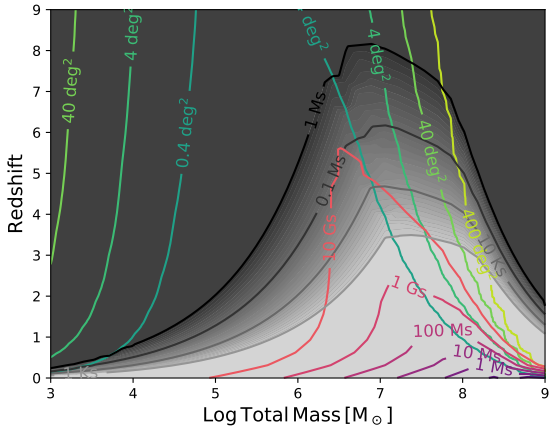


Figure 4. Same as Fig. 1, but now for the top 10% of the LISA best localised massive black hole binaries.

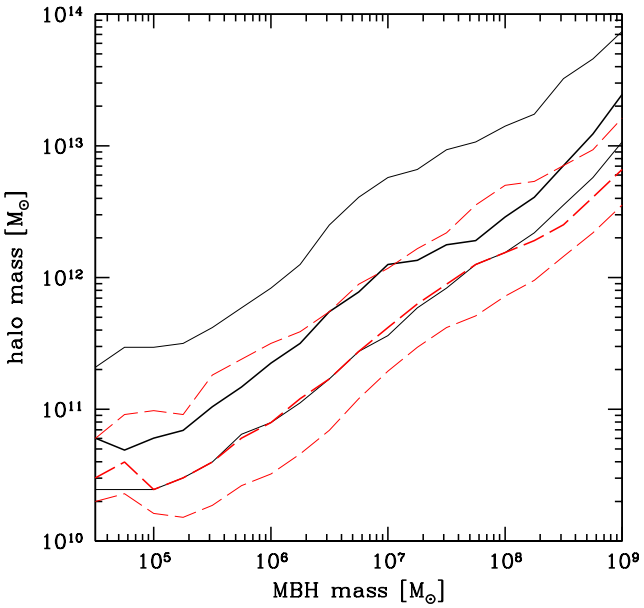


Figure 5. The median (middle curve), tenth (top curve) and ninetieth (bottom curve) percentiles of the host DM halo distribution as a function of MBHB total mass for all mergers at redshift $z < 1$ (black lines) and $2 < z < 3$ (red lines).

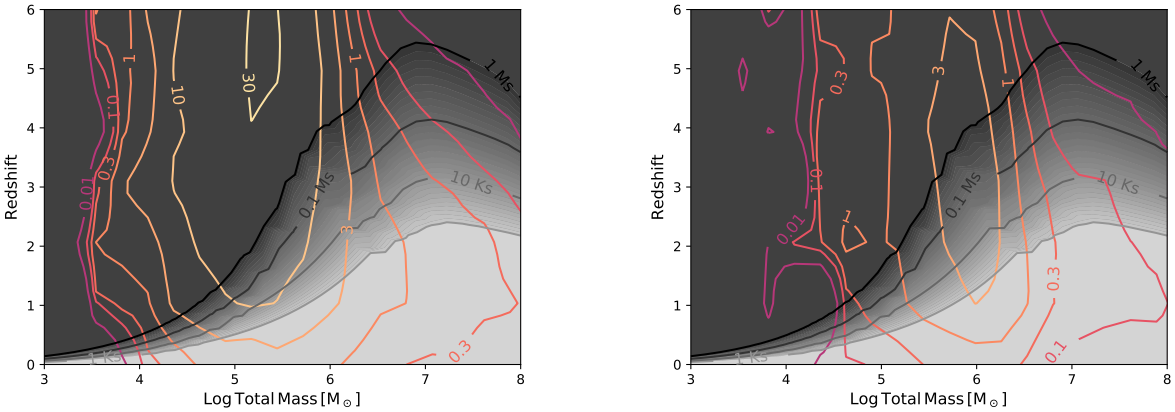


Figure 6. The median number of LISA-detected sources (for a 4 year mission duration) per unit logarithmic total mass and unit redshift, $d^2N/(d\log Mdz)$ (yellow-red contours) in the total mass-redshift plane for the model Q3 of Klein et al. (2016) without (left) and with (right) MBHB merger delay due to the hardening phase, overlaid to the integration time (grey shaded region) for Athena to detect a 10% Eddington limited accretion on the black hole remnant.

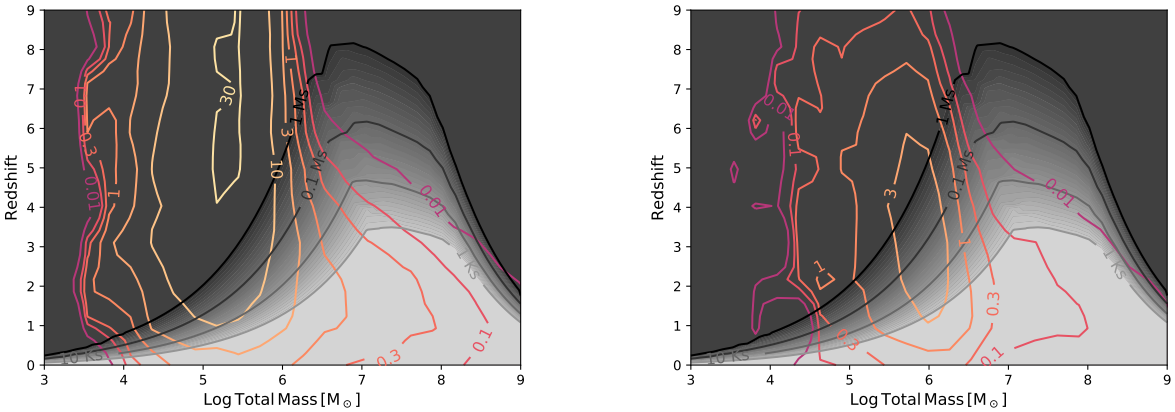


Figure 7. Same as Fig. 6, but now showing the top 10%, in terms of LISA sky localisation, of the sources.